DOI: 10.61782/fa.2025.0377

FORUM ACUSTICUM EURONOISE 2025

EXPERIMENTAL INVESTIGATION OF ROTOR SHIELDING EFFECTS ON AXIAL FLOW FAN USING AN INTERSTAGE ARRAY

Manju ADHIKARY[1,2*] **Antonio PEREIRA**[1]
Marc JACOB[1] **Ricardo BLAZQUEZ-NAVARRO**[2]
Johan THISSE[2]
[1] Ecole Centrale de Lyon, CNRS, Universite Claude Bernard Lyon 1, INSA Lyon, LMFA, UMR5509, 69130, Ecully, France
[2] AIRBUS OPERATIONS SAS, 316 Route de Bayonne, 31060 Toulouse, France

ABSTRACT

An experimental investigation is performed on a small-scale axial flow fan in a ducted configuration to observe rotor shielding effects. The study focuses on spinning azimuthal modes incident on a rotor-stator layout in the presence of flow. The sources considered are a ring of loudspeakers generating a particular spinning mode. Along with the reflection and modified transmission, several phenomena like mode scattering and mode trapping are expected. An array of 64 microphones is employed in the interstage, i.e. between the rotor and stator rows. The microphones are arranged in two rings and two spirals on the duct surface using a remote probe configuration and its axial extent is 40mm. The interstage array helps in providing a detailed understanding of the noise propagation between the rotor-stator rows. The modal decomposition is based on a Bayesian inversion method. Both the frequency dependence and the spin direction are examined at various engine operating points.

Keywords: rotor shielding, interstage array, experimental studies, axial fan

***Corresponding author**: *manju.adhikary@ec-lyon.fr.*

1. INTRODUCTION

Despite considerable advancement in the recent years to reduce noise emission by aircraft, fan noise remains to be one of the major contributors of noise generated by aircraft engines during all phases of operation. Several studies have been conducted to model the sound generation mechanisms in an engine and the free-field propagation [1, 2]. However, the study of noise transmission inside turbofan engines poses some specific challenges owing to the presence of complex geometries and heterogenous flow, and in turn, multiple noise generation and propagation mechanisms. One of the main noise source mechanisms is the rotor-wake and stator interaction noise, that generates Tyler and Sofrin modes [3]. The noise radiates in both upstream and downstream directions. A deeper understanding of the noise transmission through the rotor blades is therefore crucial for enabling more accurate assessments of noise.

One of the first analytical models to study noise transmission through static rotor blades was proposed by Kaji and Okazaki [4, 5] known as 'Cascade theory'. The blades are modelled as a cascade of finite chord length and infinitesimal blade thickness. The angle of incidence of the propagating waves has been shown to influence the reflection and transmission coefficients across the blades. The theory was further developed by using mode-matching technique to model sound generation and propagation in outlet guide vanes [6, 7]. A comparative study of different 2D and 3D analytical approaches has been performed to estimate sound transmission across stator blades [8]. Three phenomena are described based on the direction of prop-

agation of incident waves: Venetian blind, Modal condition and Blocking condition. Experimental studies have also been performed to estimate modal amplitudes generated at the inlet of a ducted fan by inverting the modal directivity matrices [9] and also using compressed sensing based mode analysis [10]. The flow between the rotor and stator blades are characterised by swirl effects, which can alter modal behaviour. A qualitative analytical model to explain transmission of BPF tones in the swirl region and through the rotor blades have been proposed [11].
In the present study, spinning azimuthal modes are generated using a ring of loudspeakers. The propagation of these modes across rotor and stator blades are observed using microphone arrays and an iterative Bayesian Inverse Approach. The experimental setup and analysis methodology are presented in the following sections. The results and comparison of transmission loss across fan stages for different modes are presented in Sec. 3, followed by a brief conclusion.

2. METHODOLOGY AND EXPERIMENTAL SETUP

Assuming linear acoustics behavior and a stationary sound field, the complex acoustic pressure inside a hard-wall cylindrical duct with a circular or annular cross-section and in the presence of a flow, can be expressed as a weighted sum of modes as shown in Eqn. 1 [12]:

$$p(r,\theta,z,t) = \sum_{m=-\infty}^{\infty}\sum_{n=0}^{\infty}[A_{mn}^{+}e^{ik_{z,mn}^{+}z} + A_{mn}^{-}e^{ik_{z,mn}^{-}z}]f_{mn}(r)e^{im\theta}e^{i\omega t} \quad (1)$$

where A_{mn}^{+} and A_{mn}^{-} are complex-valued mode amplitudes propagating downstream and upstream respectively. The subscripts m and n are the azimuthal and radial mode orders. $f_{mn}(r)$ is a normalised modal shape factor depending on the duct's cross section (circular or annular) and hard-wall boundary conditions. The axial wavenumbers $k_{z,mn}^{\pm}$ of a particular mode (m,n) in both downstream $(^{+})$ and upstream $(^{-})$ directions in the presence of a flow of Mach number M are given by

$$k_{z,mn}^{\pm} = \frac{\mp M k_0 + \sqrt{k_0^2 - (1-M^2)k_{r,mn}^2}}{1-M^2} \quad (2)$$

where, $k_{r,mn}$ is the radial wave number of mode (m,n) obtained from the solutions of Bessel functions constituting modal shape factor $f_{mn}(r)$. The purpose of the study is to generate particular modes inside a duct and observe the behavior across different blade rows of a fan.

2.1 Experimental setup

The experimental setup consists of a circular duct with a radius of 0.085 m. A low-speed electrical HVAC (Heating, ventilation and air-conditioning) fan, henceforth known as LP3, manufactured by Safran Ventilation Systems is installed inside the duct. Modular rings are present between the rotor and the stator blades in order to increase or decrease the gap among them. A Turbulent Control Screen (TCS) upstream of the fan at the inlet minimizes inflow distortions. A vane at the end of the duct can be opened or closed as required to control the mass flow inside the duct. Pressure probes and thermo-couples are fitted before and after LP3 and venturi to measure the physical parameters in the duct during operation. The parameters of LP3 are listed below:

Rotor blades number	B	17
Stator vanes number	V	23
Diameter	ϕ	17 cm
Hub to tip ratio	R_H/R_T	0.55
Tip Mach number	M_{tip}	0.3
Maximum rotational speed	Ω_{max}	$\sim$ 10000 rpm
Maximum mass flow rate	Qm	$\sim 1\ kg\ s^{-1}$
Maximum mean axial flow velocity	U_0	$\sim 40\ m\ s^{-1}$

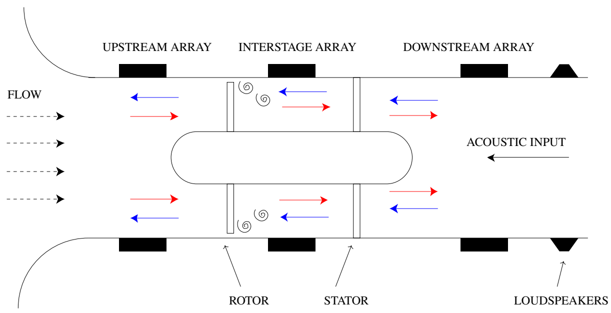

Figure 1: Schematic diagram of the experimental setup showing the positions of microphone antenna and direction of acoustic wave propagation, blue arrows depict the incident direction of modes *i.e.* the same direction as that of acoustic input and the red arrows depict the reflected direction of mode propagation

A ring of 13 loudspeakers downstream of LP3 generate a particular azimuthal mode inside the duct based on relative phase difference as explained in the methodology. The acquisition system consists of 25 nos. 1/4" microphones upstream and 25 nos. 1/4" microphones downstream with respect to the fan mounted in pin-hole configuration, and 64 nos. 1/4" microphones in the interstage mounted remotely. Fig. 1 gives a pictorial representation of the experimental setup. The fan is operated at three rotational speed and mass flow rate combinations. The performance map of the fan at these operating points are shown in Fig. 2. One of these points (9800 rpm and 30 mm vane opening) is chosen as the baseline configuration (marked with an 'o' symbol) and the corresponding results are present in the following section. The number of loudspeakers used for mode generation limits the maximum mode number that can be excited without aliasing, which is determined as half of the number of loudspeakers. Thus, for the experimental campaign modes -6 to +6 are chosen. The generation are pure tones excited individually at 30 frequencies between 500 Hz and 10000 Hz for each azimuthal mode.

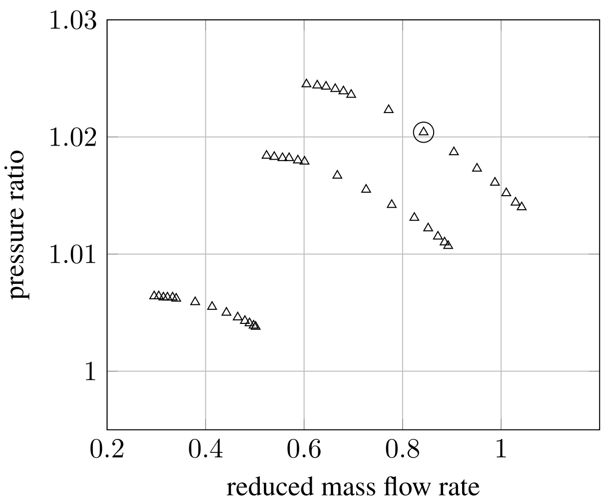

Figure 2: Performance map of the LP3 fan used in the experimentation with considered operating point marked in 'o'

2.2 Calibration of microphone arrays

The installation of the microphones on the duct is an important aspect of the experimental setup. A common method is to mount them flushed to the duct inner surface, with or without the protection grid. However, such a configuration is prone to measurement of pressure fluctuations due to turbulent boundary layer at the duct surface, along with the acoustic pressure. Furthermore, the distance between the rotor-stator rows in the long configuration is 40mm, not sufficient for flush-mounting the necessary number of microphones required for the study. Using a remote sensor installation, known as pin-hole system provides flexibility in designing a more efficient microphone array [13]. The pin-hole system creates a small cavity in front of the microphone, which acts as a Helmholtz resonator and modifies the frequency response of the microphone. Two methods of calibration are employed- individual and global calibration [14]. For individual calibration of microphones, a calibrating device consisting of a flush-mounted reference microphone and an already calibrated microphone are used. The transfer function between the target microphone and the reference microphone is measured. This is followed by the measurement of the transfer function between the reference microphone and the already calibrated microphone placed on a controlled surface. The ratio of the two transfer functions provide the calibration factor of the target microphone. The method is time-consuming and very sensitive to the position of the reference microphone in front of the pin-hole, thus difficult to reproduce. Moreover, once the setup is installed, the downstream and interstage microphones arrays are inaccessible. Therefore, individual calibration is performed for all the arrays, once before mounting the setup. Then global calibration is performed regularly during the experimental campaign. Fig. 3 gives an example of the calibration curves of microphone arrays obtained upon performing the abovementioned procedure. The curves are then used during post-processing to account for the frequency amplification and signal attenuation due to remote installation.

2.3 Mode generation

A particular spinning mode can be generated inside a duct using a combination of phased loudspeakers ([15,16]). To generate a spinning wave of azimuthal mode 'm' using 'K' monopole sources, the phase of the 'j^{th}' source is given by:

$$\phi_j = \frac{2\pi m}{K}(j-1) \tag{3}$$

The 13 loudspeakers are connected to the duct using waveguides of diameter 14 mm, resulting in a cut-off fre-

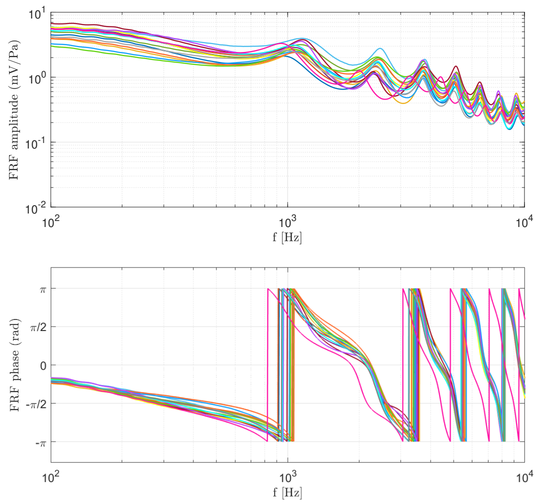

Figure 3: Sensitivity curves (amplitude and phase) for a group of microphones in the interstage array

quency of 14240.4 Hz. This ensures that the loudspeakers can be modelled as monopole sources for the range of frequencies considered in the study. The generation of radial modes cannot be controlled owing to the fact that the loudspeakers are positioned along a unique axial and radial position. The generation is performed considering a cylindrical duct, which is applicable at the position of the loudspeakers. However, at the location of the fan, notably at the Interstage array, the geometry transitions to an annular duct. It has to be noted that certain modes might become propagative, *i.e.* cut-on, as the sound propagates due to the aforementioned transition.

2.4 Analysis methodology

The iterative Bayesian Inverse Approach (iBIA) has been implemented to perform the modal analysis [17]. Eqn. 1 can be represented in a matrix notation.

$$\mathbf{p} = \mathbf{\Phi c} + \mathbf{n} \tag{4}$$

where, $\mathbf{p} \in \mathbb{C}^K$ is a vector of complex pressure coefficients (result of a Fourier transform) from measurements at a given frequency ω, $\mathbf{n} \in \mathbb{C}^K$ accounts for additive noise, $\mathbf{c} \in \mathbb{C}^L$ is a vector containing the unknown complex coefficients ($A^{\pm}_{mn}$) and $\mathbf{\Phi} \in \mathbb{C}^{K \times L}$ depends on the problem being solved ($\mathbf{\Phi} = e^{ik^{\pm}_{z,mn}z} f_{m,n}(r) e^{im\phi}$ in this case). The unknowns $\mathbf{c}$ and observations $\mathbf{p}$ are considered as random variables which are modelled through probability density functions and an algorithm based on the majorisation–minimisation (MM) principle is employed to solve the problem. Since, recorded sound pressure includes effects of the fan itself, notably when the excitation frequency is close to the blade passing frequency (BPF) or its harmonics, it is important to filter out the recorded data from these effects. To achieve that, a frequency band of 200 Hz is chosen around the excitation frequency and analysis is performed only within this range.

3. RESULTS

Upon post-processing the recorded microphone signals using the methodology explained above, the amplitudes of all cut-on modes present inside the duct are obtained. The mode amplitudes correspond to respective array locations and frequencies put to the test during the experiment. The results are presented in terms of acoustic power of the excited modes. Experiments have been conducted at specific test points. Continuous lines joining these points in the figures are for better visualisation.

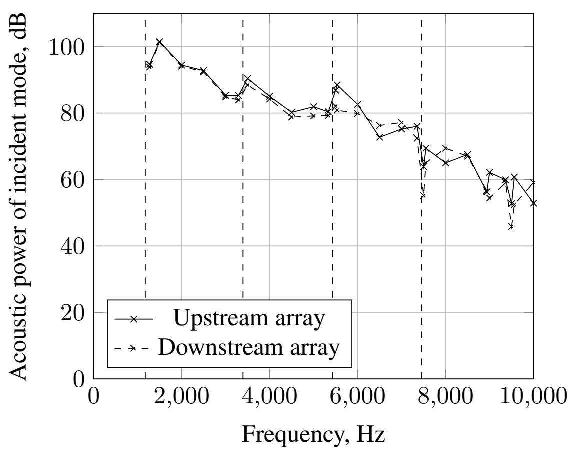

Figure 4: Acoustic power of azimuthal mode -1 (summed for all cut-on radial modes) along incident direction for upstream and downstream arrays in the case of an empty circular duct (dashed vertical lines represent the cut-off frequencies of subsequent radial modes)

For the first part of the analysis, simpler configurations have been investigated: an empty circular duct and the duct with LP3 but without rotation of blades or flow. These analyses demonstrate the performance of the methodology in conditions where the behaviour is theoretically predictable. Further, such an analysis enables the separation of the shielding due to the setup geometry from that generated due to the blades rotation and the effect of the flow. Fig. 4 presents the acoustic power of azimuthal mode -1 along the incident direction recorded by microphones of the upstream and downstream arrays. As theoretically expected, the acoustic power is conserved across the microphone arrays, specially at low frequencies where very few radial modes are cut-on. At higher frequencies, the acoustic power decrease in general and their values at upstream and downstream arrays diverge from each other. This is due to the presence of several radial modes and also spurious azimuthal modes which are excited by the loudspeakers. The method struggles to differentiate the modes, when several modes are present with comparable energy. Jumps in the power values are also observed near the cut-off frequencies of radial modes. Near the cut-off frequencies, evanescent modes with longer axial wavelength are present and recorded by the microphones. These modes have not been taken into account during the analysis. The analysis has been limited to low frequencies and test points near cut-off frequencies have been removed to ensure that observations are made within the limits of the method. Similar observations have been made for the other azimuthal modes. The results are comparable and reinforce the confidence on the generation and post-processing methodology.

The next step is to analyse the effect of the rotor rotation on the noise transmission. Fig. 5 presents an example of the results obtained when mode 1 is excited at 2000 Hz with LP3 at 9800 rpm and vane opening of 30 mm. It is the operating point marked with 'o' in Fig. 2. 'Incident' and 'reflected' represent the direction of mode propagation with respect to the acoustic input. It can be seen that the difference in amplitude of incident $m = 1$ across different antenna is negligible ($\sim$ 0.6 dB). However, the amplitude of reflected mode is considerably high at the interstage array compared to upstream array, indicating that the rotor blades are the major contributors towards reflecting $m = 1$. It can also be observed that other cut-on modes like $m = 0, -1$ are excited, however their amplitudes are negligible compared to those of $m = 1$. The overall decrease in transmission can be obtained by taking the difference of incident mode power at upstream array from that at downstream array. Fig. 6 shows the transmission loss of mode -1 with frequency for different con-

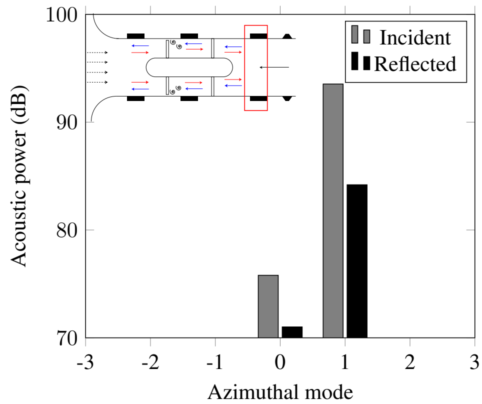

(a) Downstream array

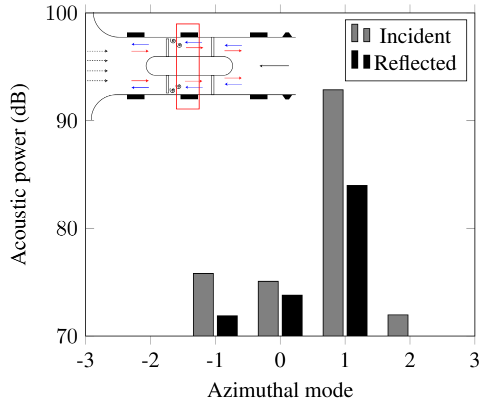

(b) Interstage array

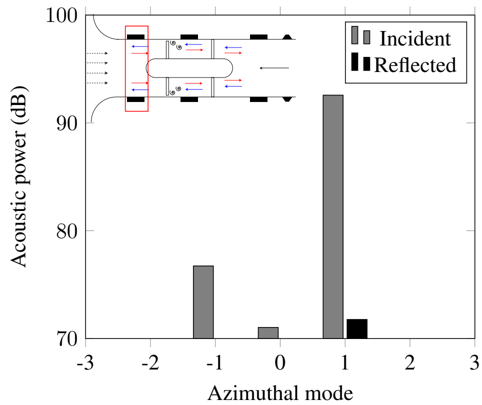

(c) Upstream array

Figure 5: Acoustic power of cut-on modes (along incident and reflected direction of propagation with respect to acoustic input) present at different microphone array locations upon excitation of azimuthal mode 1 at 2000 Hz with LP3 rotating at 9800 rpm and vane opening of 30 mm (operating point marked with 'o' in Fig. 2)

figurations. Higher difference in mode power (y-values) means lower transmission across blades. The presence of LP3 slightly decreases the transmission of mode -1. However, higher transmission loss is detected when LP3 rotates at 9800 rpm with 30 mm vane opening. The rotation of rotor blades and presence of flow are possible causes for this transmission loss. Transmission loss across each blade rows of the fan can be obtained by using the microphone measurements of interstage array. The difference in incident power of excited azimuthal mode across the downstream and interstage arrays (depicting transmission loss across stator blades) and that across the interstage and upstream arrays (depicting transmission loss across stator blades) are calculated and shown in Fig. 7 for modes $m = -1$ and $m = 1$. For the present study, $m = 1$ represents a co-rotating mode and $m = -1$ a counter-rotating mode with respect to the rotor rotation. For $m = 1$, the transmission loss across stator blades are slightly higher at low frequencies compared to rotors but above 2000 Hz, transmission loss across rotors dominate. The trend is consistent for $m = -1$, in which case, the transmission loss across rotor blades dominate throughout. The stators are slightly more efficient in blocking $m = 1$ compared to $m = -1$ but the differences are quite small and maybe accounted from the uncertainties of measurement or post-processing. However, the rotor blades are more efficient in blocking $m = -1$ upto 3 dB at 2500 Hz.

Fig. 8 shows the transmission loss across LP3 at 9800 rpm and vane opening of 30 mm for various modes. The values are obtained by taking the difference in acoustic power along incident direction of upstream array from downstream array. The lower order modes follow the trend as explained above at frequencies below 4000 Hz. With increase in frequency, transmission loss across the fan increases. However, at higher frequencies and for higher order modes, no conclusion can be drawn. It is to be noted that, along with the mode required to be excited, aliased modes are also being generated. These aliased modes are related to the number of loudspeakers present in the generation system and are given by Eq. 5.

$$m_{\text{aliased}} = m_{\text{desired}} \pm \text{Nos. of loudspeakers} \quad (5)$$

These modes are cut-on for higher order modes and thus are generated by the loudspeakers. One example of this phenomenon can be observed in Fig. 9 where mode -7 is excited along with the intended mode 6 at downstream array inside a circular duct even without LP3. The acoustic power of both these modes are comparable with a difference of ~ 1 dB. Since, both the desired and aliased modes

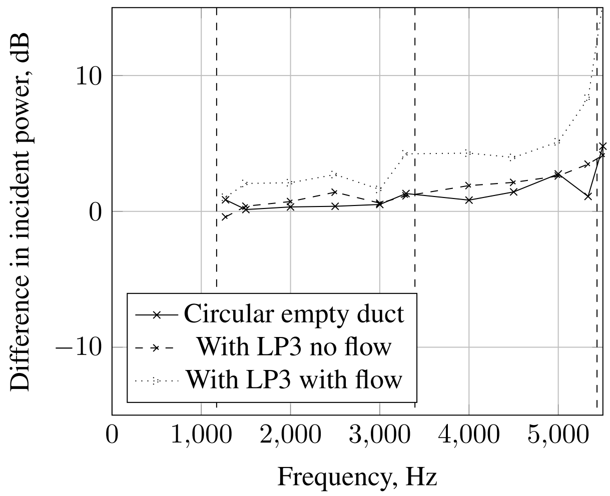

Figure 6: Difference in acoustic power along incident direction of upstream array from downstream array of azimuthal mode -1 (summed for all cut-on radial modes) for three different configurations (dashed vertical lines represent the cut-off frequencies of subsequent radial modes)

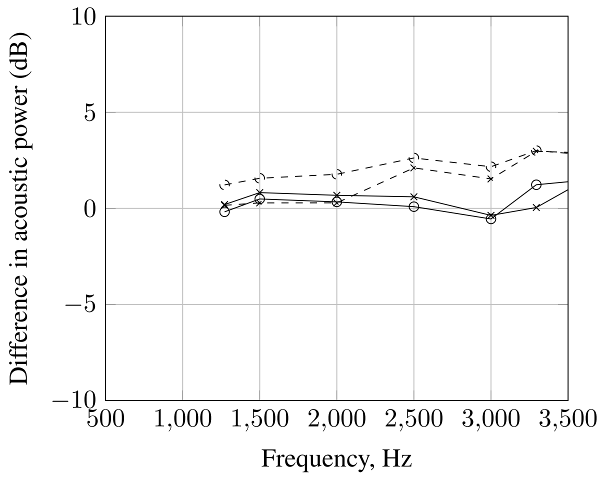

Figure 7: Difference in acoustic power of incident azimuthal mode $m = 1$ (x) and $m = -1$ (o) across stator (solid) and rotor (dashed) blades with LP3 rotating at 9800 rpm and vane opening of 30 mm

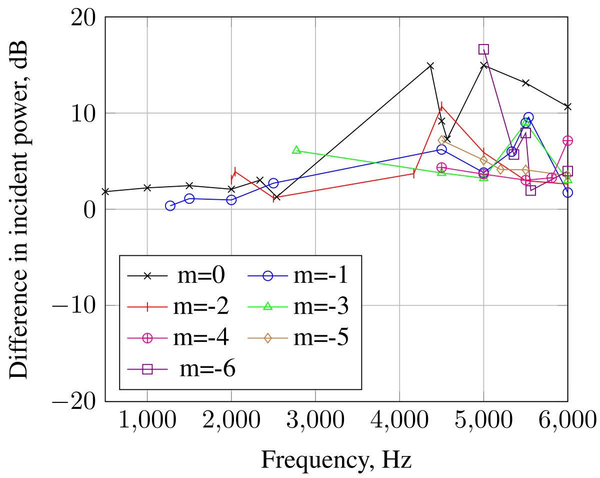

Figure 8: Difference in acoustic power along incident direction of upstream array from downstream array for different azimuthal modes (summed for all cut-on radial modes) with LP3 rotating at 9800 rpm and vane opening of 30 mm

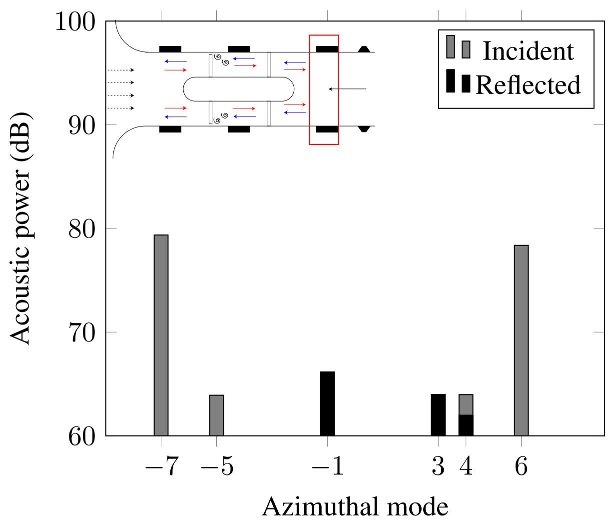

Figure 9: Acoustic power of cut-on modes (along incident and reflected direction of propagation with respect to acoustic input) present at downstream array location upon excitation of azimuthal mode 6 at 6500 Hz inside a circular duct without LP3

are generated by the same sources, they are correlated and create interference patterns inside the duct. It is possible that the energy of the aliased modes are transferred to the desired modes and vice-versa during the application of the inverse method.

4. CONCLUSION AND DISCUSSIONS

Rotor shielding across an axial fan comprising of rotor and stator blades has been studied experimentally. The analysis of lower order modes provides some information regarding rotor-shielding effects. The rotation of blades and the presence of flow increase rotor shielding effects across a fan. Stator blades are relatively transparent to the modes owing to their low stagger angles. The counter-rotating modes are shielded more efficiently by the rotor blades than the co-rotating modes. However, the analysis of higher order modes and high frequency excitation pose several challenges. It has been observed that other cut-on modes are also excited along with the desired azimuthal modes. In most cases, the mode amplitudes are considerably lower to those of the excited mode but can be comparable at certain frequencies. Due to the use of a single ring of loudspeakers, the generation of radial modes cannot be controlled. Thus, at higher frequencies and higher modes, the analysis becomes more complex and uncertain. Near the cut-off frequencies, evanescent modes are present and recorded by the microphones. Mainly at the interstage array, these modes and also the evanescent modes generated at rotor and stator edges are recorded. The evanescent modes have been ignored in the analytical formulation and thus in the modal basis of analysis. Further, the flow between the rotor and stator features swirl. For the present study, the swirl has been approximated to an equivalent axial velocity. Including the swirl effects and adding evanescent modes in the modal basis will lead to better estimation of the mode amplitudes at the interstage array. Moreover, several phenomena occur inside the experimental setup like transition from circular to annular duct, multiple reflections between rotor and stator rows and coupled effect of transmission and reflection at both the blade rows. These effects cannot be decoupled by merely investigating the mode amplitudes at microphone arrays. A numerical study is presently being conducted to simulate the experimental setup and estimate the propagation of modes across the fan. The numerical study would enable understanding of each individual phenomenon. The information will then be used to deepen the experimental analysis.

5. ACKNOWLEDGMENTS

This work was granted access to the HPC resources of PMCS2I (Pôle de Modélisation et de Calcul en Sciences de l'Ingénieur de l'Information) of École Centrale de Lyon, Écully, France. The authors acknowledge Safran Ventilation Systems and in particular, Patrice CAULE, for providing the LP3 fan-OGV module. The authors would like to thank Jean-Charles VINGIANO for the fabrication of the interstage array and mounting of the test bench. This works was performed in the framework of the Labex CeLyA (grant number ANR-10-LABX-0060) of the University of Lyon, within the program "Investissements d'Avenir" (grant number ANR-16-IDEX-0005) operated by the French National Research Agency.

6. REFERENCES

[1] W. Eversman and I. D. Roy, "Ducted Fan Acoustic Radiation Including the Effects of Nonuniform Mean Flow and Acoustic Treatments," tech. rep., NASA Lewis Research Center, 1993.

[2] M. Roger, S. Moreau, and A. Guédel, "Vortex-Shedding Noise and Potential-Interaction Noise Modeling by a Reversed Sears' Problem," in *12th AIAA/CEAS Aeroacoustics Conference, Cambridge, MA*, 2006.

[3] J. M. Tyler and T. G. Sofrin, "Axial flow compressor noise studies," *SAE Tech Papers*, 1962.

[4] S. Kaji and T. Okazaki, "Propagation of sound waves through a blade row: I. analysis based on the semi-actuator disk theory," *J. Sound Vib.*, vol. 11 (3), 1970.

[5] S. Kaji and T. Okazaki, "Propagation of sound waves through a blade row: Ii. analysis based on the acceleration potential method," *J. Sound Vib.*, vol. 11 (2), 1970.

[6] S. Bouley, B. François, M. Roger, and S. Moreau, " On a mode-matching technique for sound generation and transmission in a linear cascade of outlet guide vanes," in *21st AIAA/CEAS Aeroacoustics Conference, AIAA AVIATION Forum, Dallas, Texas*, 2015.

[7] S. Bouley, B. François, M. Roger, H. Posson, and S. Moreau, "On a two-dimensional mode-matching technique for sound generation and transmission in axial-flow outlet guide vanes," *J. Sound Vib.*, vol. 403, 2017.

[8] M. Behn, U. Tapken, P. Puttkammer, R. Hagmeijer, and N. Thouault, "Comparative study of different analytical approaches for modelling the transmission of sound waves through turbomachinery stators," in *22nd AIAA/CEAS Aeroacoustics Conference, Lyon, France*, 2016.

[9] F. O. Castres and P. F. Joseph, "Mode detection in turbofan inlets from near field sensor arrays," *J. Acoust. Soc. Am.*, vol. 121 (2), 2007.

[10] M. Behn and U. Tapken, "Investigation of Sound Generation and Transmission Effects Through the ACAT1 Fan Stage using Compressed Sensing-based Mode Analysis," in *25th AIAA/CEAS Aeroacoustics Conference, Delft, The Netherlands*, 2019.

[11] D. A. Topol, S. C. Holhubner, and D. C. Mathews, "A reflection mechanism for aft fan tone noise from turbofan engines," in *11th AIAA Aeroacoustics Conference, Palo Alto, California*, 1987.

[12] M. L. Munjal, *Acoustics of ducts and mufflers: with application to exhaust and ventilation system design*. Wiley-Interscience, 1 ed., 1987.

[13] E. Salze, C. Bailly, O. Marsden, E. Jondeau, and D. Juvè, "An experimental characterisation of wall pressure wavevector-frequency spectra in the presence of pressure gradients," in *20th AIAA/CEAS Aeroacoustics Conference, no. 2909*, (Atlanta, GA), 2014.

[14] Q. Leclère, A. Pereira, A. Finez, and P. Souchotte., "Indirect calibration of a large microphone array for in-duct acoustic measurements," *J. Sound Vib.*, vol. 376, 2016.

[15] J. M. Seiner and G. Reethof, "Design and Development of the Spinning Mode Synthesizer," tech. rep., National Aeronautics and Space Administration, 1973.

[16] S. Huang, X. Pan, L. Yu, and W. Jiang, "Achieving cylindrical duct modes generation in spinning mode synthesizer via a least-square identification of the global calibration factor," *Appl Acoust*, vol. 186, 2022.

[17] A. Pereira and M. Jacob, "Modal analysis of in-duct fan broadband noise via an iterative bayesian inverse approach," *J. Sound Vib.*, vol. 520, no. 116633, 2022.